The anti-tumor effects of Mfn2 in breast cancer are dependent on promoter DNA methylation, the P21^{Ras} motif and PKA phosphorylation site

YUFENG LI[1], WENYUE DONG[2], XIJIN SHAN[3], HUI HONG[4], YAN LIU[5], YANKUN LIU[1], XIAOHUI LIU[6], XIAOJUN ZHANG[7] and JINGHUA ZHANG[1]

[1]The Cancer Institute; [2]Department of Anesthesiology, Affiliated Tangshan People's Hospital of North China University of Science and Technology, Tangshan, Hebei 063001; [3]Department of Surgery, Rizhao Port Hospital, Rizhao, Shandong 276800; [4]Department of Head, Neck and Breast Surgery, Shangrao People's Hospital, Shangrao, Jiangxi 334000; [5]Department of Bioengineering, College of Life Sciences, North China University of Science and Technology, Tangshan, Hebei 063000; [6]Department of Thoracic Surgery, Affiliated Tangshan People's Hospital of North China University of Science and Technology, Tangshan, Hebei 063001; [7]Department of Internal Medicine, Affiliated Zunhua People's Hospital of North China University of Science and Technology, Zunhua, Hebei 064200, P.R. China

Received March 18, 2017; Accepted February 8, 2018

DOI: 10.3892/ol.2018.8314

Abstract. Mitofusin 2 (*Mfn2*) is expressed in numerous human tissues and serves a pivotal role in cell proliferation. However, Mfn2 is considered as an anti-tumor gene, and is silenced in human malignant tumors, including those of breast cancer. However, the mechanisms contributing to *Mfn2* silencing and the mechanism of its anti-tumor function in breast cancer remain unclear. In the present study, hypoexpression of *Mfn2,* and hypermethylation of its promoter, was confirmed in human breast cancer cells and in breast cancer tissues by reverse transcription-quantitative polymerase chain reaction (PCR) and methylation specific PCR, respectively. Chemical demethylation treatment with 5-aza-2'-deoxycytidine upregulated the mRNA expression level of *Mfn2* in MCF-7 cells in a dose-dependent manner. In addition, overexpression of *Mfn2* repressed the proliferation, migration and invasion of MCF-7 cells, mediated by inhibition of the Ras-extracellular signal-regulated kinase (ERK)1/2 signaling pathway. However, overexpression of *Mfn2* with deletion of the p21^{Ras} motif (*Mfn2*$^{\Delta Ras}$) and protein kinase A (PKA) phosphorylation site (*Mfn2*$^{\Delta PKA}$) partially reduced the anti-tumor function of Mfn2, and inhibited the Ras-ERK1/2 signaling pathway. Taken together, the present study confirmed the anti-tumor effects of Mfn2 in human breast cancer and clarified that the mechanism of its anti-tumor functions includes promoter DNA methylation, the P21^{Ras} binding site and PKA phosphorylation.

Correspondence to: Professor Xiaojun Zhang, Department of Internal Medicine, Affiliated Zunhua People's Hospital of North China University of Science and Technology, 316 Huaming Road, Zunhua, Hebei 064200, P.R. China
E-mail: tech_ol@foxmail.com

Dr Jinghua Zhang, The Cancer Institute, Affiliated Tangshan People's Hospital of North China University of Science and Technology, 65 Shengli Road, Tangshan, Hebei 063001, P.R. China
E-mail: jhzhang_sc@sina.com

Abbreviations: Mfn2, mitofusin 2; PKA, protein kinase A; HSG, hyperperplasia suppressor gene

Key words: human breast cancer, mitofusin 2, DNA methylation, Ras-extracellular signal-regulated kinase 1/2 signaling pathway

Introduction

Breast cancer is among the most common types of cancer, which affects women of all age groups worldwide (1). The mortality rate of breast cancer has remained ~20% for 5 years (1). This is likely due to the fact that the complex molecular mechanisms of breast cancer pathology remain to be fully understood. The elucidation of these mechanism is an important requirement to improve the treatment available for breast cancer (2).

Mitofusin 2 (*Mfn2*), also named hyperperplasia suppressor gene (*HSG*), is expressed in numerous human tissues and serves a pivotal role in the proliferation and apoptosis of vascular smooth muscle cells (VSMCs) (3,4). However, *Mfn2* has been demonstrated to be hypoexpressed in various types of human malignant tumors, including gastric cancer, hepatocellular cancer, colorectal cancer, urinary bladder cancer and breast cancer (5-9). Therefore, *Mfn2* is considered a cancer suppressor gene, and elucidation of its anti-tumor mechanism may contribute to cancer therapy.

DNA methylation is an essential epigenetic mechanism required for control of gene expression. Methylation usually occurs at CpG sites in gene promoters mediated by DNA methyltransferases (DNMTs) (10,11). Generally, 70-80% CpG sites in the human genome are methylated (12). Abnormal

DNA methylation is a common event in human cancers, including hypermethylation of a tumor suppressor gene, hypomethylation of an oncogene and global hypomethylation of the genome (13-15). DNA methylation is a reversible process, making it a promising target for cancer therapy.

It is well established that the structure of a protein determines its biological function. It has been demonstrated that rat Mfn2 protein contains a $p21^{Ras}$ signature motif (amino acids 77-92) and a PKA phosphorylation site at Ser442 (3). The $p21^{Ras}$ motif and PKA phosphorylation site are necessary for the anti-proliferative effect of Mfn2 on rat vascular smooth muscle cells (VSMCs) (3,16). The human homolog shares 95.2% similarity with the rat Mfn2 amino acid sequence (3). In the present study, the DNA methylation status of the *Mfn2* promoter was analyzed in breast cancer cells and tissues, as well as the effect of demethylation on *Mfn2* expression. Furthermore, the importance of the $p21^{Ras}$ motif and PKA phosphorylation site at Ser 442 for the anti-proliferation and anti-invasion effects of Mfn2 in breast cancer was also demonstrated. The present study will provide a novel viewpoint for understanding the anti-tumor function of Mfn2 in human breast cancer.

Materials and methods

Tissue specimens. The 7 pairs of fresh breast cancer tissue and adjacent non-tumor tissue were obtained from patients (25-55 years old) who underwent breast surgery in the Tangshan People's Hospital (Tangshan, China) between March 2011 and March 2012. A distance of ~5 cm was required between the adjacent non-tumor tissues and the tumor tissue boundary. The selected tumor tissues were confirmed by pathologists to contain >80% tumor cells. None of the patients had undergone preoperative chemotherapy, radiotherapy and/or other treatments. The protocol and use of the specimens in the present study was approved by the Institutional Ethics Committee of Tangshan People's Hospital (Tangshan, China), and written consent was obtained from all participants.

Cell lines. The human breast cancer cell line, MCF-7, was purchased from the Cell Resource Center of the Institute of Basic Medicine, Chinese Academy of Medical Sciences (Beijing, China). The cells were cultured in DMEM medium (Thermo Fisher Scientific, Inc., Waltham, MA, USA) supplemented with 10% fetal bovine serum (FBS; Hyclone, GE Healthcare Life Sciences, Logan, UT, USA) at 37˚C with 5% CO_2. To demethylate cell DNA, the MCF-7 cells were treated with 0, 5, 10 and 15 μM 5-aza-2'-deoxycytidine (5-aza-CdR) for 5 consecutive days. The 5-aza-CdR is a cytidine analog that can incorporate into DNA during S phase and disrupt the interaction between DNA and DNMT. The culture medium was replaced every 48 h. Untreated cells were used as a control.

Plasmids and transfection. pEGFP-N1 plasmids expressing the complete *Mfn2* open reading frame, the *Mfn2* with $p21^{ras}$ signature motif deletion mutant ($Mfn2^{\Delta Ras}$) and protein kinase A (PKA) phosphorylation site deletion ($Mfn2^{\Delta PKA}$) were purchased from Shanghai GenePharma Co., Ltd. (Shanghai, China). The pEGFP-N1 plasmid (Promega Corporation, Madison, WI, USA) was used as control. The MCF-7 cells were seeded in 6-well plates ($2x10^5$/well) and cultured for 24 h. Subsequently, the cells were respectively transfected with the pEGFP-N1, $Mfn2^{\Delta Ras}$ and $Mfn2^{\Delta PKA}$ plasmids (4 μg/2 ml) using Lipofectamine® 2000 Reagent (Thermo Fisher Scientific, Inc., Waltham, MA, USA), according to the manufacturer's protocol.

RNA extraction and reverse transcription-quantitative polymerase chain reaction (RT-qPCR). Total RNA was extracted from human tissue samples and cultured cells (48 h post-transfection) using TRIzol (Thermo Fisher Scientific, Inc.), according to the manufacturer's instructions, and concentration was determined by NanoDrop 2000 (Thermo Fisher Scientific, Inc.). Reverse transcription was performed using 2 μg total RNA with a Reverse Transcriptase First Chain cDNA kit (Takara Bio, Inc., Otsu, Japan). The *Mfn2* mRNA expression level was determined by RT-qPCR using a SYBR-Green Master Mix kit and PikoReal 96 RT-PCR system (Thermo Fisher Scientific, Inc.). PCR was performed in triplicate and each experiment was repeated 3 times. The primer sequences used are as follows: *Mfn2*, forward, 5'-TTCCACAAGGTG AGTGAGC-3', and reverse, 5'-TTAGCAGACACAAAGAAG ATGC-3'; Cyclin D1, forward, 5'-CCGTCCATGCGGAAG ATC-3', and reverse, 5'-ATGGCCAGCGGGAAGAC-3'; GADPH, forward, 5'-GAGAGGGAAATCGTGCGTGAC-3', and reverse, 5'-CATCTGCTGGAAGGTGGACA-3'. GAPDH was used as an internal control. The PCR condition was set to 94˚C for 3 min; followed by 30 cycles of 94˚C for 30 sec, 60˚C for 30 sec and 70˚C for 60 sec; and a final extension step at 72˚C for 5 min. The $2^{-\Delta\Delta Cq}$ method (17) was used to analyze the relative changes in *Mfn2* expression.

Methylation-specific PCR (MSPCR). The genomic DNAs of cells and human tissue samples were extracted with 10 mg/ml proteinase K (Amresco, LLC, Solon, OH, USA) digestion at 55˚C for 15 min (cells) and 3 h (human tissue). Subsequently, the purification was performed. Phenol: Chloroform: Isoamyl alcohol (25:24:1; Tianjing Baishi Chemical Industry Co., Ltd., Tianjin, China) was added and vortexed thoroughly for 20 sec followed by centrifugation at room temperature for 5 min at 16,000 x g. After upper aqueous phase was removed, the layer was transferred to a fresh tube and was used for isopropyl alcohol (Tianjin Fuyu Fine Chemicals Co., Ltd., Tianjin, China) precipitation. The extracted DNA samples were stored in TE buffer at -20˚C until use. Bisulfite-based DNA modification, which converts all unmethylated cytosine bases to uracil, was performed using a Methylcode Bisulfite Conversion kit (Thermo Fisher Scientific, Inc.), according to the manufacturer's instructions. HotStar Taq DNA polymerase (Fermentas; Thermo Fisher Scientific, Inc.) was used for the PCR reaction. The modified DNA was used as a template for MSPCR with primers specific for either the modified-methylated or unmethylated *Mfn2* gene promoter sequences. PCR amplification was performed with the following primer sets, which include the CpG island of *Mfn2*: methylated forward, 5'-TGGTTTTGA ATTTTCGATGTATTC-3', methylated reverse, 5'-CAAAAC AATAAACACTAACCCGTA-3'; unmethylated forward, 5'-GGTTTTGAATTTTTGATGTATTTGT-3', unmethylated reverse, 5'-CAAAACAATAAACACTAACCACATA-3'. The

PCR amplification program consisted of 10 min at 95˚C hen followed by 40 cycles of denaturation for 30 sec at, annealing for 30 sec at 60˚C, extension for 30 sec at 72˚C, and a final extension at 72˚C for 10 min. The PCR products were separated on 1.5% agarose gels with DuRed Nucleic acid dye (Beijing Fanbo Biochemicals Co., Ltd., Beijing, China) and visualized under ultraviolet illumination.

Western blot analysis. Total protein was collected using protein lysis buffer containing 1 mM phenylmethylsulfonyl fluoride protease inhibitor and centrifugation at 14,000 x g for 30 min at 4˚C. Protein concentration in the supernatant was determined by BCA assay (Beijing Solarbio Science & Technology Co., Ltd., Beijing, China), according to the manufacturer's protocol. A total of 45 μM protein was dissolved in loading buffer (Beijing Solarbio Science & Technology Co., Ltd., Beijing, China), and denatured by heating at 100˚C for 5 min. The proteins were then separated by 10% SDS-PAGE Following separation, the proteins were transferred onto an immunoblot polyvinylidene difluoride membrane (Thermo Fisher Scientific, Inc.). The protein bands were confirmed by 0.2% Ponceau S staining for 5 min at room temperature. Membranes were blocked with 5% BSA (Sigma-Aldrich; Merck KGaA; Darmstadt, Germany) for 2 h at 37˚C, then incubated with the following primary antibodies overnight at 4˚C: Anti-*Mfn2* (0.5 μg/ml; cat. no. ab50838), anti-Cyclin D1 (1:100; cat. no. ab16663), anti-p-ERK (1:50; cat. no. ab223500), anti-ERK (1:500; cat. no. ab17942), anti-GAPDH (1:1,000; cat. no. ab9485) and anti-β-Actin (1:1,000; cat. no. ab8227; all Epitomics; Abcam, Cambridge, UK). The membranes were washed 3 times in Tris-buffered saline solution with Tween-20 (1X TBST) and incubated with horseradish peroxidase-conjugated goat-anti-rabbit antibody (Beijing Solarbio Science & Technology Co., Ltd.; 1:500; cat. no. SE134) for 1 h at 37˚C. Following a final wash with 1X TBST, immunoreactive bands were detected using the ChampGel automatic gel imaging analyzer (Beijing Sage Creation Science Co., Ltd., Beijing, China). Optical band density was quantified using ImageJ (version 1.44p; National Institutes of Health, Bethesda, MD, USA).

Cell proliferation assays. Cell proliferation assays were performed using Cell Counting Kit-8 (CCK-8; Dojindo Molecular Technologies, Inc., Kumamoto, Japan), according to the manufacturer's instructions. The cells were seeded into 96-well microtiter plates at a density of $7.0x10^3$ cells/well and cultured for 24 h. The cells were then treated with increasing concentrations of 5-aza-CdR (0, 5, 10, 15 μM) for 5 days. Subsequently, 10 μl CCK-8 solution was added to each well. The absorbance was measured at 450 nm using a microplate reader, and a calibration curve was prepared using the data obtained from standardized wells that contained known numbers of viable cells. Each experiment was performed in 5 replicate wells and repeated 3 times independently.

Cell cycle analysis. Flow cytometry was performed for cell cycle analysis. The cells were seeded into 6-well plates and treated with increasing concentrations of 5-aza-CdR (0, 5, 10, 15 μM) for 1, 2 and 3 days. Subsequently, the treated and untreated cells were washed with PBS followed and fixed in ice-cold 70% ethanol in PBS for 24 h at 4˚C. Subsequent to another wash, the fixed cells were treated with 0.01% RNase (Sigma-Aldrich; Merck KGaA) for 10 min at 37˚C, and then stained with 0.05% propidium iodide for 20 min at 4˚C in the dark. The cell cycle distribution was determined using a FACSCanto flow cytometry system (Becton Dickinson; BD Biosciences, Franklin Lakes, NJ, USA), and analyzed with Modfit 3.2 software (Verity Software House, Inc., Topsham, ME, USA; http://www.vsh.com). The experiment was repeated 3 times.

Scratch wound assay. MCF-7 cells were cultured in 6-well plates until ~95% confluent. Then, a scratch wound was created using a 200-μl pipette tip. The wounded cells were washed twice with culture medium to remove the detached cells, then replaced in DMEM medium supplemented with 10% FBS at 37˚C with 5% CO_2. Images of the wounds were acquired using a digital camera 24 h after the wounds were made. Wound width (μm) was measured using a standard caliper, and the experiment was performed in triplicate, repeated ≥3 times.

Transwell invasion assay. The cell invasion capability was detected using transwell chamber culture systems (pore diameter, 8-μm; Corning Incorporated, Corning, NY, USA). A total of $2x10^4$ cells were placed onto a Matrigel-coated transwell chamber with serum-free opti-MEM medium (Thermo Fisher Scientific, Inc.). The DMEM medium containing 10% FBS was added to the lower chamber as a chemoattractant. After 24 h, the cells attached to the lower surface of the insert filter were counted using 0.1% crystal violet staining for 20 min at room temperature. The images were captured using an Olympus IX71 fluorescent microscope equipped with an Olympus DP73 digital camera (both Olympus Corporation, Tokyo, Japan).

Statistical analysis. All statistical analysis was performed using SPSS software version 13.0 (SPSS, Inc., Chicago, IL, USA). The data are presented as the mean ± standard deviation. One-way analysis of variance was used to analyze differences between groups. Scheffe post hoc testing was used to determine pairwise differences between means. $P<0.05$ was considered to indicate a statistically significant difference.

Results

Hypoexpression of Mfn2 and hypermethylation of its promoter in breast cancer. The mRNA expression level of *Mfn2* was analyzed in 7 pairs of human breast cancer and adjacent non-tumor tissues using RT-qPCR. As demonstrated in Fig. 1A, *Mfn2* was hypoexpressed in breast cancer tissues compared with the corresponding adjacent non-tumor tissues ($P<0.05$). Given that DNA methylation is associated with gene expression, the methylation level of *Mfn2* promoter was analyzed by MSPCR, with the aim of clarifying the mechanism behind *Mfn2* silencing in breast cancer. Using the MethPrimer tool, 1 typical CpG island was identified in the upstream promoter of *Mfn2*. As demonstrated in Fig. 1B, the *Mfn2* promoter was hypermethylated in the majority of breast tumor tissues (6/7) compared with the corresponding adjacent non-tumor tissues. These data indicate that silencing of *Mfn2*

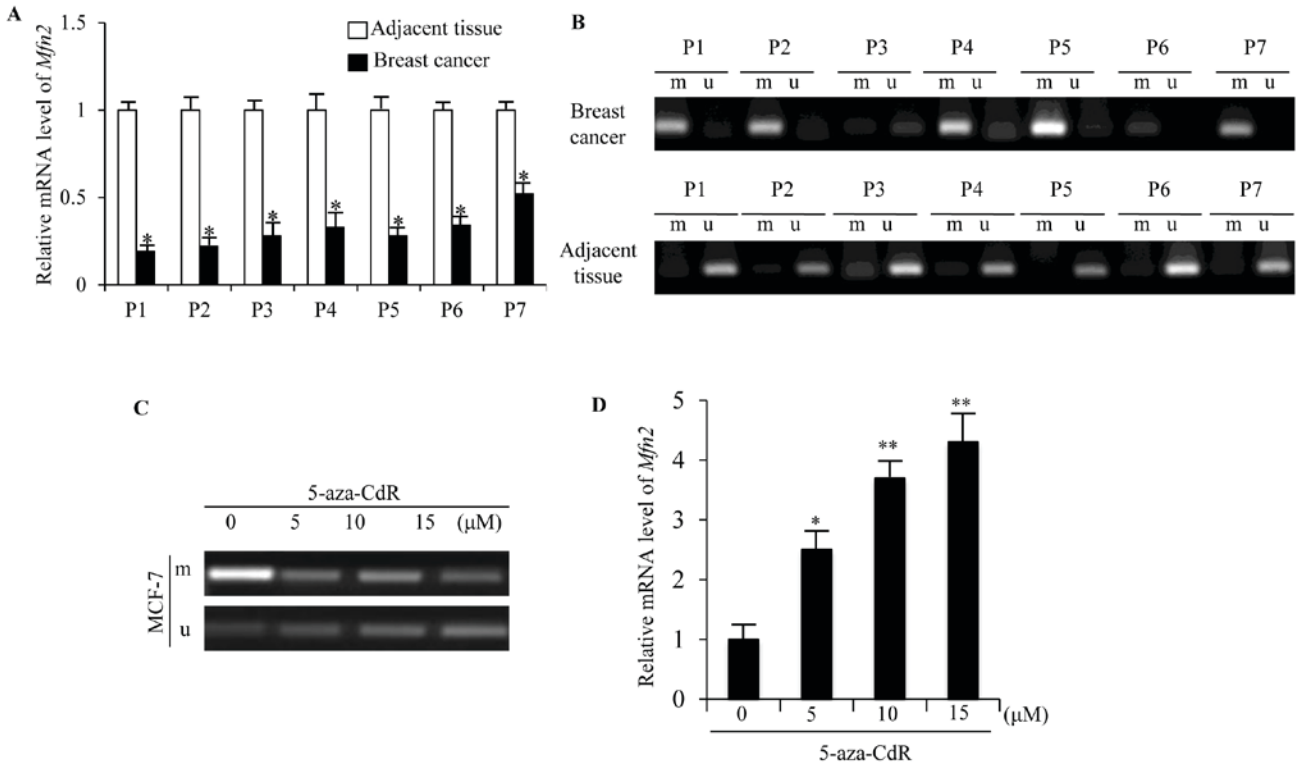

Figure 1. mRNA expression and promoter methylation status of *Mfn2* in human breast cancer. (A) mRNA expression of *Mfn2* in human breast cancer relative to the matched adjacent non-tumor tissues from 7 patients (P1-P7) were analyzed by RT-qPCR with *GAPDH* as an internal control. *P<0.05 vs. matched adjacent non-tumor tissue. (B) Methylation statuses of *Mfn2* promoter in breast cancer and adjacent non-tumor tissues were analyzed by methylation-specific polymerase chain reaction. (C) Methylation statuses of the *Mfn2* promoter in MCF-7 cells treated with 5-aza-CdR at 5, 10 and 15 μM for 5 days. (D) The mRNA expression of *Mfn2* in MCF-7 cells treated with 5, 10 and 15 μM 5-aza-CdR, determined by RT-qPCR with *GAPDH* as an internal control. The results are expressed as the mean ± standard deviation. *P<0.05 and **P<0.01 vs. untreated cells. Mnf2, mitofusin 2; RT-qPCR, reverse transcription-quantitative polymerase chain reaction; 5-aza-CdR, 5-aza-2'-deoxycytidine; m, methylated PCR product; u, unmethylated PCR product.

by DNA hypermethylation on its promoter may contribute to the tumorigenesis of breast cancer. *Mfn2* may be a tumor suppressor gene in breast cancer.

Demethylation treatment of MCF-7 cells. DNA methylation is a reversible process, making it a promising target for cancer therapy. 5-aza-CdR is widely used as an inhibitor of DNMTs and can increase the expression of genes silenced by DNA methylation (18-21). In order to confirm whether the expression of *Mfn2* in human breast cancer cells is regulated by DNA methylation of its promoter, the MCF-7 breast cancer cells were treated with 5-aza-CdR for 1, 2 and 3 days at concentrations of 5.0 10 and 15 μM. The methylation level of the *Mfn2* promoter in the 5-aza-CdR-treated groups decreased in a dose-dependent manner compared with the untreated group (Fig. 1C). Conversely, the mRNA expression levels of *Mfn2* in the 5-aza-CdR-treated groups increased in a dose-dependent manner compared with that of the untreated group (P<0.05; Fig. 1D). These data indicate that demethylation treatment could upregulate *Mfn2* expression in breast cancer.

Overexpression of Mfn2 inhibits growth, migration and invasion of MCF-7 cells. To clarify the anti-tumor role of Mfn2 in breast cancer, the MCF-7 cells were transfected with pEGFP-N1-*Mfn2* plasmids for 48 h, producing ~85% GFP-positive cells (data not shown). The overexpression of *Mfn2* in MCF-7 cells transfected with N1-*Mfn2* were confirmed by RT-qPCR (P<0.01; Fig. 2A) and immunoblot analysis (P<0.01; Fig. 2B). Compared with the control cells (N1), the proliferation ability of *Mfn2*-overexpressing MCF-7 cells was markedly decreased (P<0.05; Fig. 2C), and the cell cycle was mostly arrested in G0/G1 phase (P<0.05; Fig. 2D). This suggests that the growth suppression effect of *Mfn2* may be the result of inhibition of the cell cycle. In addition, the migration and invasion abilities of MCF-7 cells overexpressing *Mfn2* were markedly inhibited compared with the control cells, as detected by the wound assay (P<0.05; Fig. 2E) and the invasion assay (P<0.05; Fig. 2F). These data suggest that overexpression of *Mfn2* could suppress the growth and metastasis of breast cancer.

The anti-proliferation, anti-migration and anti-invasion effects of Mfn2 are mediated by the Ras-Raf-ERK1/2 signaling pathway. It was reported that Mfn2 could bind to Ras protein with its $p21^{Ras}$ motif in rat VSMCs (3). The anti-proliferative effect of Mfn2 on VSMCs was mediated by inhibition of the Ras-Raf-ERK1/2 signaling pathway. Deletion of the $p21^{Ras}$ motif abolished Mfn2-induced growth arrest of VSMCs. Due to the 95% homology of the amino acid sequence of Mfn2 in rats and humans, it was speculated that *Mfn2* may interact with Ras via the $p21^{Ras}$ motif in human breast cancer cells. To test this hypothesis, MCF-7 cells were transfected with plasmids containing the *Mfn2* open reading frame (ORF) lacking the $p21^{Ras}$ coding sequence ($Mfn2^{\Delta Ras}$). As demonstrated in Fig. 2A and B, the mRNA and protein expression

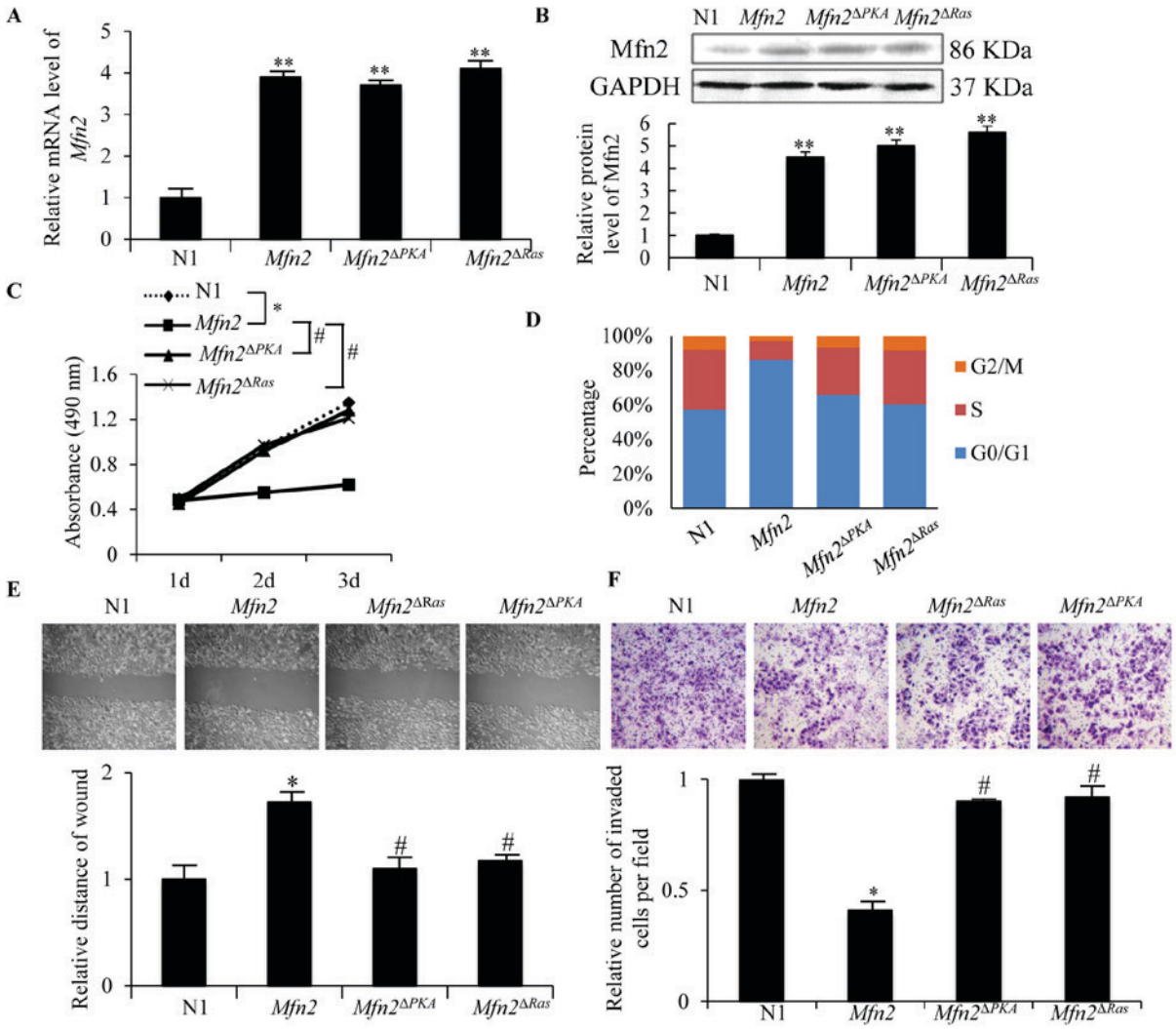

Figure 2. Proliferation, migration and invasion abilities of MCF-7 cells transfected with N1, *Mfn2*, $Mfn2^{\Delta Ras}$ and $Mfn2^{\Delta PKA}$ plasmids. (A) The mRNA level of *Mfn2* in each group was detected by reverse transcription-quantitative polymerase chain reaction 24 h post-transfection, using *GAPDH* as internal control. The data are presented as expression relative to that of N1. (B) Mfn2 protein expression was detected by western blotting 48 h post-transfection. Quantification of the protein band was analyzed by Image Pro Plus software. (C) Cells of each group were seeded into 96 plates at $7.0x10^3$/well. Cell proliferation was detected using a Cell counting kit-8 assay for 3 days. The data are representative of 3 experiments. (D) Cells were seeded in a 25 cm^2 tissue culture flask and harvested at 80% confluence for cell cycle distribution analysis by flow cytometry. (E) Migration activity was detected using a scratch wound assay. x100, magnification. The bar graph demonstrates the fold change of wound distance relative to N1. (F) Invasion ability was analyzed using a transwell assay with Matrigel. The cells attached to the lower surface of the insert were stained with crystal violet, imaged and counted in 5 random fields of view (x200, magnification). The data represent the mean ± standard deviation of the number of cells relative to the N1 group in 3 experiments. *P<0.05 and **P<0.01 vs. N1 group; $^\#$P<0.05 vs. *Mfn2* group. N1, EGFP-N1 plasmid; *Mfn2*, mitofusin 2; $Mfn2^{\Delta Ras}$, *Mfn2* ORF lacking the $p21^{Ras}$ coding sequence; $Mfn2^{\Delta PKA}$, *Mfn2* ORF lacking the protein kinase A phosphorylation site coding sequence.

levels of *Mfn2* in MCF-7 cells transfected with $Mfn2^{\Delta Ras}$ plasmids were not significantly different from cells transfected with *Mfn2* full length plasmids. However, the proliferation (P<0.05) (Fig. 2C), migration (Fig. 2E) and invasion (Fig. 2F) abilities of MCF-7 cells transfected with $Mfn2^{\Delta Ras}$ plasmids were markedly increased compared with those of MCF-7 cells transfected with Mfn2 full length plasmids (P<0.05). The cell cycle arrest was also rescued (Fig. 2D). Thus, the anti-proliferation, anti-migration and anti-invasion functions of $Mfn2^{\Delta Ras}$ were partially abolished, indicating that the $p21^{Ras}$ motif of Mfn2 is required for it anti-tumor effects in breast cancer and that Mfn2 probably serves a role in regulating the Ras-Raf-MEK-ERK1/2 signaling cascade.

The protein expression level of ERK1/2, a major downstream signaling protein of Ras, and activated phosphorylated ERK1/2 (p-ERK1/2) were detected. As demonstrated in the Fig. 3A, the protein level of p-ERK1/2 was markedly decreased by overexpression of *Mfn2*, but not $Mfn2^{\Delta Ras}$ (P<0.05). Given that Ras-ERK1/2 signaling has been demonstrated to induce *Cyclin D1* expression to modulate the G1-S phase transition (22), the expression of *Cyclin D1* was also analyzed. The mRNA and protein expression levels of *Cyclin D1* were significantly downregulated in MCF-7 cells transfected with *Mfn2* compared with control cells (P<0.05; Fig. 3B and C). This suggests that Mfn2-induced cell-cycle arrest in the G0/G1 phases is attributable, at least in part, to inhibition of the Ras-ERK1/2-cyclin D1 pathway. Deletion of the $p21^{Ras}$ motif partially abolished Mfn2-induced inhibition of ERK1/2 phosphorylation (Fig. 3A) and expression of *Cyclin D1* (Fig. 3B and C), indicating a crucial interaction between Mfn2 and Ras in breast cancer cells.

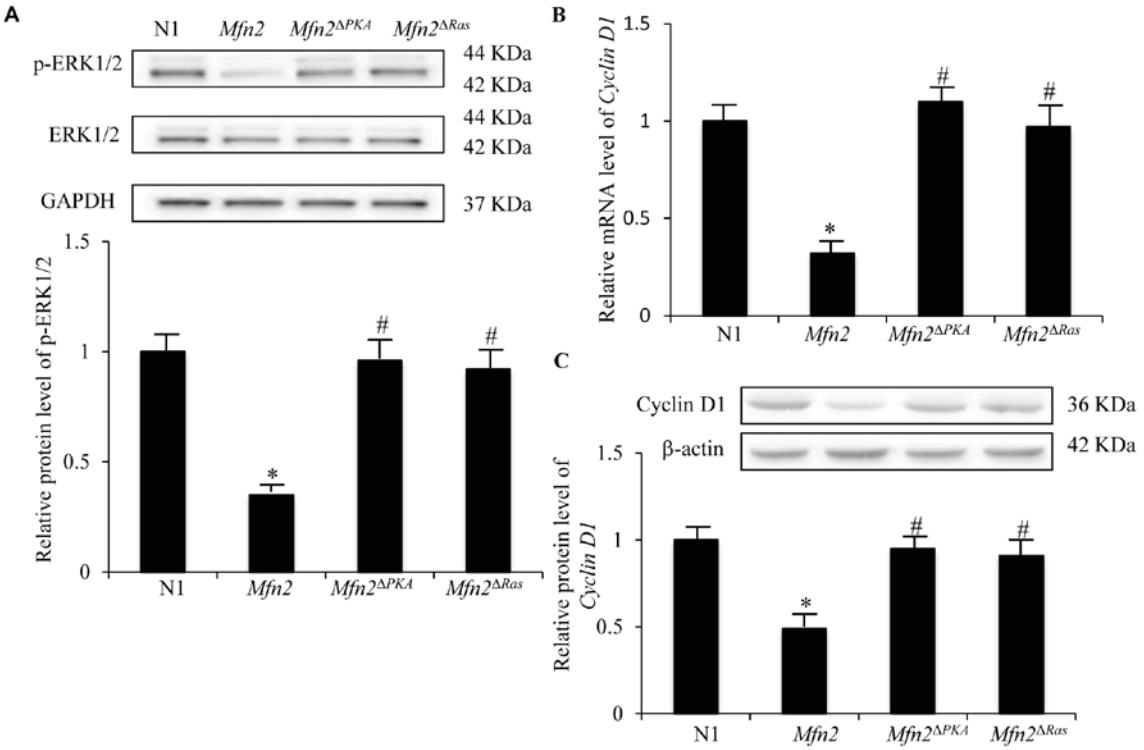

Figure 3. Expression of p-ERK and Cyclin D1 in MCF-7 cells transfected with N1, *Mfn2*, $Mfn2^{\Delta Ras}$ and $Mfn2^{\Delta PKA}$ plasmids. (A) Protein expression levels of ERK and p-REK in determined by western blotting, using GAPDH as a control. The results are expressed as the mean ± standard deviation. *P<0.05 vs. N1 group; $^{\#}$P<0.05 vs. *Mfn2* group. (B) mRNA expression of *Cyclin D1* determined by reverse transcription-quantitative polymerase chain reaction, relative to the N1 group, using *GAPDH* as an internal control. (C) Relative protein expression levels of *Cyclin D1* determined by western blotting using β-actin as a control. Showed. Results are expressed as the mean ± standard deviation of 3 experiments, relative to the N1 group. *P<0.05 vs. N1 group; $^{\#}$P<0.05 vs. *Mfn2* group. p-, phosphorylated; ERK1/2, extracellular signal-regulated kinase 1/2; N1, EGFP-N1 plasmid; *Mfn2*, mitofusin 2; $Mfn2^{\Delta Ras}$, *Mfn2* ORF lacking the $p21^{Ras}$ coding sequence; $Mfn2^{\Delta PKA}$, *Mfn2* ORF lacking the protein kinase A phosphorylation site coding sequence.

The PKA site phosphorylation of Mfn2 is also required for its anti-proliferation, anti-migration and anti-invasion functions. It has been established that Ser442 of Mfn2 is a protein kinase A (PKA) phosphorylation site (4). The PKA site of Mfn2 is essential for Mfn2-mediated inhibition of ERK1/2 signaling, and the consequent anti-proliferative effect, in rat VSMCs (16). In order to evaluate the importance of the PKA site of Mfn2 in human breast cancer, MCF-7 cells were transfected with plasmids containing the *Mfn2* ORF with a PKA phosphorylation site deletion ($Mfn2^{\Delta PKA}$). A total of 48 h post-transfection, the mRNA and protein expression levels of *Mfn2* in MCF-7 cells transfected with $Mfn2^{\Delta PKA}$ plasmids were not significantly different to those of MCF-7 cells transfected with *Mfn2* full length plasmids (Fig. 2A and B). However, the proliferation (Fig. 2C), migration (Fig. 2E) and invasion (Fig. 2F) abilities of MCF-7 cells transfected with $Mfn2^{\Delta PKA}$ plasmids were markedly increased compared with cells transfected with *Mfn2* full length plasmids (P<0.05). Cell cycle arrest was also rescued (Fig. 2D). This indicates that the PKA phosphorylation site was necessary for the anti-proliferation, anti-migration and anti-invasion functions of the Mfn2 protein. Furthermore, the expression levels of p-ERK1/2 (Fig. 3A) and Cyclin D1 (Fig. 3B and C) were significantly increased in MCF-7 cell transfected with $Mfn2^{\Delta PKA}$ plasmids compared with those in MCF-7 cells transfected with Mfn2 full length plasmids (P<0.05). These data indicate a crucial role of the PKA phosphorylation site of Mfn2 in the inhibition of the Ras-ERK1/2-Cyclin D1 pathway.

Discussion

The present study confirmed that *Mfn2* was hypoexpressed, and its promoter was hypermethylated, in the MCF-7 cell line and in human breast cancer specimens. However, Sorianello *et al* (23) reported that the promoter of *Mfn2* was unmethylated in rat insulinoma and hepatoma cells, as analyzed by bisulfite sequencing. It is speculated that *Mfn2* expression is regulated via different mechanisms which vary between species and tissues. In addition, demethylation treatment of MCF-7 cells with 5-aza-CdR resulted in upregulation of *Mfn2* expression in a dose-dependent manner. This suggests that *Mfn2* hypoexpression in breast cancer is at least partially attributable to hypermethylaton of its promoter. Although 5-aza-CdR can rescue the expression of tumor suppressor genes by demethylating their promoter CpG sites (24-31), its clinical anti-tumor applications are limited due to lack of gene specificity. Furthermore, it was reported that *Mfn2* is a direct target of miR-761 and upregulation of *Mfn2* expression by inhibiting miR-761 repressed hepatocarcinoma growth and metastasis (32). These results indicate that epigenetic mechanisms serve an important role in regulating *Mfn2* expression at a transcriptional and post-transcriptional level.

It has been established that the drosophila, rat and human homologues of HSG serve a critical role in mitochondrial fusion (33-36). In the present study, the anti-proliferation, anti-migration and anti-invasion effects of Mfn2 were confirmed in breast cancer cells. The results are consistent with previous studies in VSMCs (3) and in various types of cancer, including breast cancer (18,37) gastric cancer (18), urinary bladder carcinoma (38) and hepatocellular carcinoma (20,21,23) and lung adenocarcinoma (5,8,24,38-41). However, tumor-promoting functions of Mfn2 in lung adenocarcinoma have also been reported (42,43). These conflicting results may be due to differing experimental methods, but suggest that the roles of Mfn2 in different types of cancer are more complicated than expected.

Furthermore, the effect of Mfn2 protein structure of on its function in breast cancer was analyzed. In rat VSMCs, the $p21^{Ras}$ motif of *Mfn2* serves an essential role in Mfn2-mediated inhibition of ERK1/2 signaling and growth arrest (33-36). In the present study, it was demonstrated that the $p21^{Ras}$ motif of Mfn2 is also necessary for its anti-proliferation function in breast cancer cells. Mfn2-Ras binding negatively regulated the Ras-ERK1/2-cyclin D1 signaling pathway and resulted in cell cycle arrest in the G0/G1 phases of breast cancer cells. This suggests that Mfn2 is an important protein in the Ras-signaling pathway. Furthermore, it is known that Mfn2 contains a PKA phosphorylation site at Ser442 (33-36) and the cAMP-PKA signaling pathway is a versatile signal pathway involved in regulation of cellular functions through phosphorylation (44-48). The present study demonstrated that the PKA phosphorylation site at Ser442 of Mfn2 was essential for Mfn2-mediated inhibition of ERK1/2 signaling and reduced proliferation of breast cancer cells. These results support those demonstrated in VSMCs (16,33-36). It was speculated that deletion of the PKA phosphorylation site at Ser442 of Mfn2 affects its tertiary structure and, consequently, its interaction with Ras.

Although the absence of the $p21^{Ras}$ motif or the PKA phosphorylation site at Ser442 of Mfn2 has no effect on its mitochondrial membrane localization (3), altered mitochondrial function in breast cancer has been observed (49). In breast cancer cells, with the overexpression of *Mfn2*, the vesicular endocytosis-associated protein, SH3 domain-containing GRB2-like protein 2 (SH3GL2), was demonstrated to translocate to mitochondria, and induce the production of superoxide and the release of cytochrome C from the mitochondria to the cytoplasm (49). This was accompanied by decreased lung and liver metastases and primary tumor growth (49). SH3GL2 depletion reversed this phenotype (49). This indicates that the anti-tumor functions of Mfn2 are also mitochondrial-dependent.

To conclude, the present study demonstrates that *Mnf2* functions as a suppressor of breast cancer and suggests that elucidation of its complex mechanism may reveal a novel target for breast cancer therapy.

Acknowledgements

The authors would like to thank Dr Hongmei Liu at Tangshan People's Hospital (Tangshan, China) for providing the 5-aza-CdR.

Funding

The present study was partially supported by the National Natural Science Foundation of China (grant no. 81301779).

Availability of data and materials

The raw data are available from the corresponding author on reasonable request.

Authors' contributions

JZ and XZ designed the experiments and revised the manuscript. YL analyzed the data and wrote the manuscript. WD, XS, HH, XL, YanL and YankL performed the experiments. All authors discussed the results and commented on the manuscript.

Ethics approval and consent to participate

The protocol and use of the specimens in the present study was approved by the Institutional Ethics Committee of Tangshan People's Hospital (Tangshan, China), and written consent was obtained from all participants.

Consent for publication

Written informed consent for the publication was obtained from all patients.

Competing interests

The authors declare that they have no competing interests.

References

1. DeSantis CE, Lin CC, Mariotto AB, Siegel RL, Stein KD, Kramer JL, Alteri R, Robbins AS and Jemal A: Cancer treatment and survivorship statistics, 2014. CA Cancer J Clin 64: 252-271, 2014.
2. Fojo T: Multiple paths to a drug resistance phenotype: Mutations, translocations, deletions and amplification of coding genes or promoter regions, epigenetic changes and microRNAs. Drug Resist Updat 10: 59-67, 2007.
3. Chen KH, Guo X, Ma D, Guo Y, Li Q, Yang D, Li P, Qiu X, Wen S, Xiao RP and Tang J: Dysregulation of HSG triggers vascular proliferative disorders. Nat Cell Biol 6: 872-883, 2004.
4. Zhang D, Ma C, Li S, Ran Y, Chen J, Lu P, Shi S and Zhu D: Effect of Mitofusin 2 on smooth muscle cells proliferation in hypoxic pulmonary hypertension. Microvasc Res 84: 286-296, 2012.
5. Zhang GE, Jin HL, Lin XK, Chen C, Liu XS, Zhang Q and Yu JR: Anti-tumor effects of Mfn2 in gastric cancer. Int J Mol Sci 14: 13005-13021, 2013.
6. Wang W, Sun Q, Wu Z, Zhou D, Wei J, Xie H, Zhou L and Zheng S: Mitochondrial dysfunction-related genes in hepatocellular carcinoma. Front Biosci (Landmark Ed) 18: 1141-1149, 2013.
7. Jin B, Fu G, Pan H, Cheng X, Zhou L, Lv J, Chen G and Zheng S: Anti-tumour efficacy of mitofusin-2 in urinary bladder carcinoma. Med Oncol 28 (Suppl 1): S373-S380, 2011.
8. Ma L, Liu Y, Geng C, Qi X and Jiang J: Estrogen receptor β inhibits estradiol-induced proliferation and migration of MCF-7 cells through regulation of mitofusin 2. Int J Oncol 42: 1993-2000, 2013.
9. Xia Y, Wu YQ, Zhang L, Li XL, Yuan HL, He XJ, Tao DD, Gong JP and Qiu FZ: Effects of mitofusin-2 gene on proliferation and chemosensitivity of human breast carcinoma cell line MCF-7. Ai Zheng 26: 815-819, 2007 (In Chinese).

10. Jones PA: Functions of DNA methylation: Islands, start sites, gene bodies and beyond. Nat Rev Genet 13: 484-492, 2012.
11. Chik F and Szyf M: Effects of specific DNMT gene depletion on cancer cell transformation and breast cancer cell invasion; toward selective DNMT inhibitors. Carcinogenesis 32: 224-232, 2011.
12. Antequera F and Bird A: Number of CpG islands and genes in human and mouse. Proc Natl Acad Sci USA 90: 11995-11999, 1993.
13. Bergman Y and Cedar H: DNA methylation dynamics in health and disease. Nat Struct Mol Biol 20: 274-281, 2013.
14. Akhavan-Niaki H and Samadani AA: DNA methylation and cancer development: Molecular mechanism. Cell Biochem Biophys 67: 501-513, 2013.
15. Kanwal R and Gupta S: Epigenetic modifications in cancer. Clin Genet 81: 303-311, 2012.
16. Zhou W, Cao WJ, Chen LL, Xiaomei G and Guanghui CH: Effect of mitofusin 2 gene with protein kinase A phosphorylation site deletion on the proliferation of vascular smooth muscle cells. J Clin Rehabilitative Tissue Engineering Res 14: 1322-1325, 2010.
17. Livak KJ and Schmittgen TD: Analysis of relative gene expression data using real-time quantitative PCR and the 2(-Delta Delta C(T)) method. Methods 25: 402-408, 2001.
18. Gnyszka A, Jastrzebski Z and Flis S: DNA methyltransferase inhibitors and their emerging role in epigenetic therapy of cancer. Anticancer Res 33: 2989-2996, 2013.
19. Yoo CB and Jones PA: Epigenetic therapy of cancer: Past, present and future. Nat Rev Drug Discov 5: 37-50, 2006.
20. Lee S, Kim HS, Roh KH, Lee BC, Shin TH, Yoo JM, Kim YL, Yu KR, Kang KS and Seo KW: DNA methyltransferase inhibition accelerates the immunomodulation and migration of human mesenchymal stem cells. Sci Rep 5: 8020, 2015.
21. Xu J, Huo D, Chen Y, Nwachukwu C, Collins C, Rowell J, Slamon DJ and Olopade OI: CpG island methylation affects accessibility of the proximal BRCA1 promoter to transcription factors. Breast Cancer Res Treat 120: 593-601, 2010.
22. Guo Y, Stacey DW and Hitomi M: Post-transcriptional regulation of cyclin D1 expression during G2 phase. Oncogene 21: 7545-7556, 2002.
23. Sorianello E, Soriano FX, Fernandez-Pascual S, Sancho A, Naon D, Vila-Caballer M, Gonzalez-Navarro H, Portugal J, Andres V, Palacin M and Zorzano A: The promoter activity of human Mfn2 depends on Sp1 in vascular smooth muscle cells. Cardiovasc Res 94: 38-47, 2012.
24. Vucic EA, Brown CJ and Lam WL: Epigenetics of cancer progression. Pharmacogenomics 9: 215-234, 2008.
25. Tada M, Kanai F, Tanaka Y, Tateishi K, Ohta M, Asaoka Y, Seto M, Muroyama R, Fukai K, Imazeki F, *et al*: Down-regulation of hedgehog-interacting protein through genetic and epigenetic alterations in human hepatocellular carcinoma. Clin Cancer Res 14: 3768-3776, 2008.
26. Duffy MJ, Napieralski R, Martens JW, Span PN, Spyratos F, Sweep FC, Brunner N, Foekens JA and Schmitt M; EORTC PathoBiology Group: Methylated genes as new cancer biomarkers. Eur J Cancer 45: 335-346, 2009.
27. Tost J, Hamzaoui H, Busato F, Neyret A, Mourah S, Dupont JM and Bouizar Z: Methylation of specific CpG sites in the P2 promoter of parathyroid hormone-related protein determines the invasive potential of breast cancer cell lines. Epigenetics 6: 1035-1046, 2011.
28. Caffarelli E and Filetici P: Epigenetic regulation in cancer development. Front Biosci (Landmark Ed) 16: 2682-2694, 2011.
29. Coppedè F: The role of epigenetics in colorectal cancer. Expert Rev Gastroenterol Hepatol 8: 935-948, 2014.
30. Milavetz BI and Balakrishnan L: Viral epigenetics. Methods Mol Biol 1238: 569-596, 2015.
31. Wu Y, Sarkissyan M and Vadgama JV: Epigenetics in breast and prostate cancer. Methods Mol Biol 1238: 425-466, 2015.
32. Zhou X, Zhang L, Zheng B, Yan Y, Zhang Y, Xie H, Zhou L, Zheng S and Wang W: MicroRNA-761 is upregulated in hepatocellular carcinoma and regulates tumorigenesis by targeting Mitofusin-2. Cancer Sci 107: 424-432, 2016.
33. Santel A and Fuller MT: Control of mitochondrial morphology by a human mitofusin. J Cell Sci 114: 867-874, 2001.
34. Rojo M, Legros F, Chateau D and Lombès A: Membrane topology and mitochondrial targeting of mitofusins, ubiquitous mammalian homologs of the transmembrane GTPase Fzo. J Cell Sci 115: 1663-1674, 2002.
35. Karbowski M, Lee YJ, Gaume B, Jeong SY, Frank S, Nechushtan A, Santel A, Fuller M, Smith CL and Youle RJ: Spatial and temporal association of Bax with mitochondrial fission sites, Drp1, and Mfn2 during apoptosis. J Cell Biol 159: 931-938, 2002.
36. Chen H, Detmer SA, Ewald AJ, Griffin EE, Fraser SE and Chan DC: Mitofusins Mfn1 and Mfn2 coordinately regulate mitochondrial fusion and are essential for embryonic development. J Cell Biol 160: 189-200, 2003.
37. Stefansson OA, Jonasson JG, Olafsdottir K, Hilmarsdottir H, Olafsdottir G, Esteller M, Johannsson OT and Eyfjord JE: CpG island hypermethylation of BRCA1 and loss of pRb as co-occurring events in basal/triple-negative breast cancer. Epigenetics 6: 638-649, 2011.
38. Wang W, Zhu F, Wang S, Wei J, Jia C, Zhang Y, Zhou L, Xie H and Zheng S: HSG provides antitumor efficacy on hepatocellular carcinoma both in vitro and in vivo. Oncol Rep 24: 183-188, 2010.
39. Xia Y, Wu Y, He X, Gong J and Qiu F: Effects of mitofusin-2 gene on cell proliferation and chemotherapy sensitivity of MCF-7. J Huazhong Univ Sci Technolog Med Sci 28: 185-189, 2008.
40. Wang W, Zhou D, Wei J, Wu Z, Cheng X, Sun Q, Xie H, Zhou L and Zheng S: Hepatitis B virus X protein inhibits p53-mediated upregulation of mitofusin-2 in hepatocellular carcinoma cells. Biochem Biophys Res Commun 421: 355-360, 2012.
41. Rehman J, Zhang HJ, Toth PT, Zhang Y, Marsboom G, Hong Z, Salgia R, Husain AN, Wietholt C and Archer SL: Inhibition of mitochondrial fission prevents cell cycle progression in lung cancer. FASEB J 26: 2175-2186, 2012.
42. Lou Y, Li R, Liu J, Zhang Y, Zhang X, Jin B, Liu Y, Wang Z, Zhong H, Wen S and Han B: Mitofusin-2 over-expresses and leads to dysregulation of cell cycle and cell invasion in lung adenocarcinoma. Med Oncol 32: 132, 2015.
43. Lou Y, Zhang Y, Li R, Gu P, Xiong L, Zhong H, Zhang W and Han B: Transcriptional profiling revealed the anti-proliferative effect of MFN2 deficiency and identified risk factors in lung adenocarcinoma. Tumour Biol 37: 8643-8655, 2016.
44. Ansurudeen I, Willenberg HS, Kopprasch S, Krug AW, Ehrhart-Bornstein M and Bornstein SR: Endothelial factors mediate aldosterone release via PKA-independent pathways. Mol Cell Endocrinol 300: 66-70, 2009.
45. Martini CN, Plaza MV and Vila Mdel C: PKA-dependent and independent cAMP signaling in 3T3-L1 fibroblasts differentiation. Mol Cell Endocrinol 298: 42-47, 2009.
46. Omar B, Zmuda-Trzebiatowska E, Manganiello V, Göransson O and Degerman E: Regulation of AMP-activated protein kinase by cAMP in adipocytes: Roles for phosphodiesterases, protein kinase B protein kinase A, Epac and lipolysis. Cell Signal 21: 760-766, 2009.
47. McConnachie G, Langeberg LK and Scott JD: AKAP signaling complexes: Getting to the heart of the matter. Trends Mol Med 12: 317-323, 2006.
48. Lorenowicz MJ, Fernandez-Borja M, Kooistra MR, Bos JL and Hordijk PL: PKA and Epac1 regulate endothelial integrity and migration through parallel and independent pathways. Eur J Cell Biol 87: 779-792, 2008.
49. Kannan A, Wells RB, Sivakumar S, Komatsu S, Singh KP, Samten B, Philley JV, Sauter ER, Ikebe M, Idell S, *et al*: Mitochondrial reprogramming regulates breast cancer progression. Clin Cancer Res 22: 3348-3360, 2016.